ACS Catalysis

pubs.acs.org/acscatalysis Research Article

Double-Carrousel Mechanism for Mn-Catalyzed Dehydrogenative Amide Synthesis from Alcohols and Amines

Jesús A. Luque-Urrutia, Tània Pèlachs, Miquel Solà,* and Albert Poater*

Cite This: *ACS Catal.* 2021, 11, 6155–6161 Read Online

ACCESS | Metrics & More | Article Recommendations | Supporting Information

ABSTRACT: We study with density functional theory calculations the mechanism of the original example of a base-metal-catalyzed synthesis of amides from alcohols and amines. A preliminary proposal of the mechanism of this reaction was experimentally reported by Milstein and co-workers. Instead of the proposed reaction mechanism with a hemilabile pincer amine arm, our DFT calculations describe a facile protocol, where the catalyst only produces aldehydes from alcohols. Once formaldehyde is formed from methanol, it reacts with the amine to form a second alcohol. This new alcohol undergoes the same procedure as methanol and creates the desired amide through a double-carrousel mechanism. The rate-determining step in the catalytic aldehyde synthesis corresponds to the H_2 formation. However, in the nonmetal-catalyzed part of the mechanism, the interaction of formaldehyde with the amine is also quite kinetically demanding.

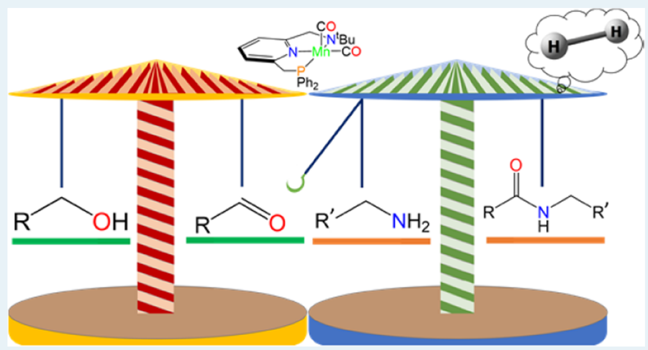

KEYWORDS: *aldehyde, acceptorless dehydrogenative coupling, amide, alcohol, manganese catalyst*

■ INTRODUCTION

In the third decade of the third millennium, there is a fever to develop efficient electric cars[1] with the aim to reduce pollution in large cities, and, in general, to alleviate the greenhouse effect,[2] apart from the ozone depletion.[3] Among the main culprits are carbon dioxide (CO_2) and nitrous oxide (N_2O) generated by the burning of fossil fuels.[4−6] We can use experiments[7] and theory[8] to generate ways to fix both CO_2 and N_2O,[9] but also pull toward hydrogen (H_2) generation, to avoid their undesired production.

It has been believed that the ideal source of hydrogen production could be the environmentally friendly oxidation of water, but such an approach is still far from efficient; thus, alternatives must be sought. The process called acceptorless dehydrogenative coupling (ADC) of alcohols,[10] with organic substrates, such as alkenes,[11] amines,[12,13] or nitriles,[14,15] is one of such alternatives. In these reactions, the involved hydrogen atoms do not become part of any subsequent organic molecule but are simply free as byproducts. These processes might become a potential way to convert alcohol via molecular hydrogen as the main fuel in the future,[10b] and these alcohols are obtained from a sustainable source such as biomass.[16] Surely, thinking of hydrogen as an energy source from this reaction is very pretentious, in quantitative terms, but this ADC process can be applied toward the development of liquid organic hydrogen carriers.[17] Returning to the origins of the ADC developed by Milstein and co-workers, ADC was first demonstrated by coupling of primary alcohols to form esters,[18] whereas the first example of amide formation by ADC of alcohols and amines was reported 2 years later.[19] Even though obtaining hydrogen in ADC reactions might be considered as a positive accident since the primary goal was to obtain an imine, or if condensation is avoided, an amide, ADC reactions represent a good example of a successful design of green chemical processes. In the synthesis of these chemicals, however, a metal complex is needed to facilitate them. This role was first played by ruthenium complexes,[18,20] followed by other precious metals,[21] and then during the last decade, it was possible to use more abundant first-row transition metals,[22] such as manganese[11,23] coordinating pincer ligands.[24]

Due to the important appearance of amides in medical treatments (they are present in about a quarter of current drugs,[25] plastics, diverse materials, and even in the DNA as a link between amino acids),[26] it is necessary to optimize the amide bond formation to reduce chemical waste and increase the production yield.[27] This line of research was followed by Milstein and co-workers who reported the first base-metal-catalyzed synthesis of amides employing primary amines with alcohols, using a pincer-based MnP^{tBu}NNH catalyst (**1**), as

Received: February 12, 2021
Revised: March 31, 2021
Published: May 6, 2021

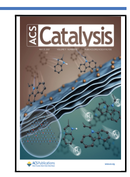

https://doi.org/10.1021/acscatal.1c00693
ACS Catal. 2021, 11, 6155–6161

shown in Figure 1. This synthetic methodology for amide synthesis avoids dealing with either carboxylic acids or their amine-activated derivatives in the presence of promoters,[28] with the corresponding undesired generation of stoichiometric amounts of residues.[29] This MnP^{t}BuNNH-type of a catalyst was shown before to catalyze the dehydrogenative coupling of amines and diols to form cyclic imides in the presence of a base.[30]

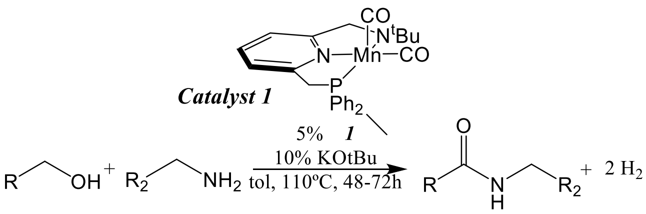

Figure 1. Mn-based catalyst involved in the dehydrogenative amide synthesis from alcohols and amines.

Catalyst **1** can convert up to 94% of alcohol into amide without the need of a promoter molecule and forming hydrogen gas as a byproduct. In the search for a plausible mechanism for the catalytic conversion schematized in Figure 1, we envisaged density functional theory (DFT) calculations. We were particularly interested in analyzing whether a plausible Mn−N bond cleavage during the process could reduce the potential of this catalyst due to possible decomposition. This cleavage was suggested in the originally proposed mechanism by Milstein et al.[13a] for the amide synthesis reaction catalyzed by **1** (see step **4**→**II** in the preliminary mechanistic proposal of Figure 2).

COMPUTATIONAL DETAILS

All DFT calculations were performed with the Gaussian 16 set of programs.[31] The electronic configuration of the molecular systems was described with the BP86 functional of Becke and Perdew,[32] using the Ahlrichs basis set def2SVP.[33] Since corrections due to dispersion are essential to study the reactivity, we have included them through Grimme's method with Becke−Johnson damping (GD3BJ keyword in Gaussian).[34,35] The geometry optimizations were performed without symmetry constraints and the characterization of the local stationary points was carried out by analytical frequency calculations. These frequencies were used to calculate unscaled zero-point energies (ZPEs) as well as thermal corrections and entropy effects at 383.15 K and 1 atm. Solvent effects were included with the polarizable continuous solvation model (PCM)[36] using toluene as a solvent in single-point energy calculations on the optimized geometries with the M06 functional[37] and the cc-pVTZ basis set.[38] The reported Gibbs energies in this work include M06/cc-pVTZ//BP86-D3BJ/Def2SVP electronic energies with solvent effects obtained at the same level of theory,[13b,15,39] corrected with zero-point energies, thermal corrections, and entropy effects evaluated at 383.15 K with the BP86-D3BJ/Def2SVP method. The resulting solvation Gibbs energies were added to the final Gibbs energies in the gas phase to obtain Gibbs energies in solution.[40] Standard Gibbs energies in a solution refer to a 1 M standard-state concentration for all species. The change of the conventional 1 atm standard state for gas-phase calculations to a standard state of 1 M concentration in a solution requires the introduction of a correction in the Gibbs energy term of 2.62 kcal/mol.[41] Finally, according to Shaik and Kozuch,[42] in most catalytic cycles, only one transition state and one intermediate determine the turnover frequency (TOF). They are called the TOF-determining transition state (TDTS) and the TOF-determining intermediate (TDI).

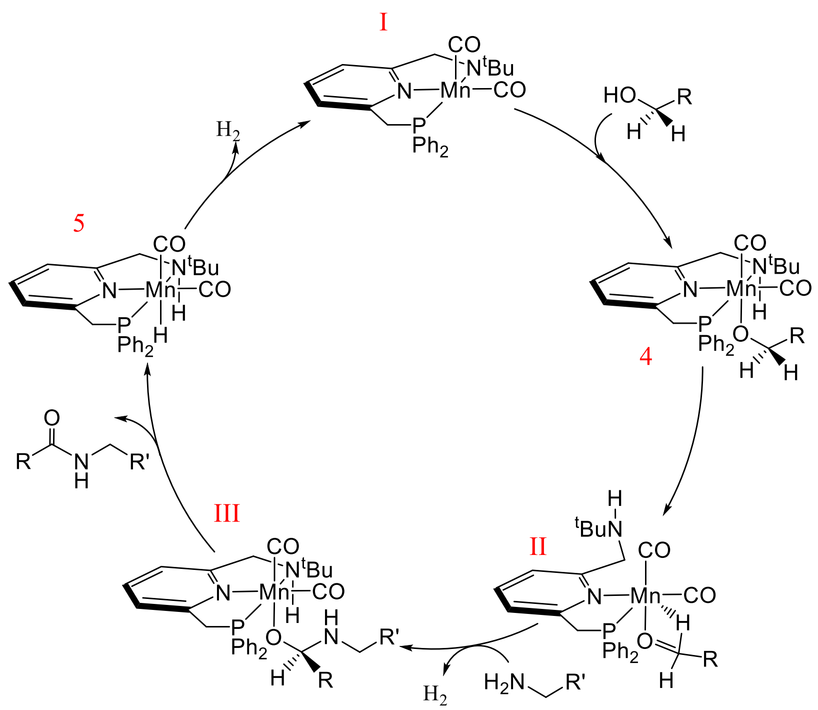

Figure 2. Initial proposed mechanism for the amide synthesis reaction catalyzed by **1**.

https://doi.org/10.1021/acscatal.1c00693
ACS Catal. 2021, 11, 6155−6161

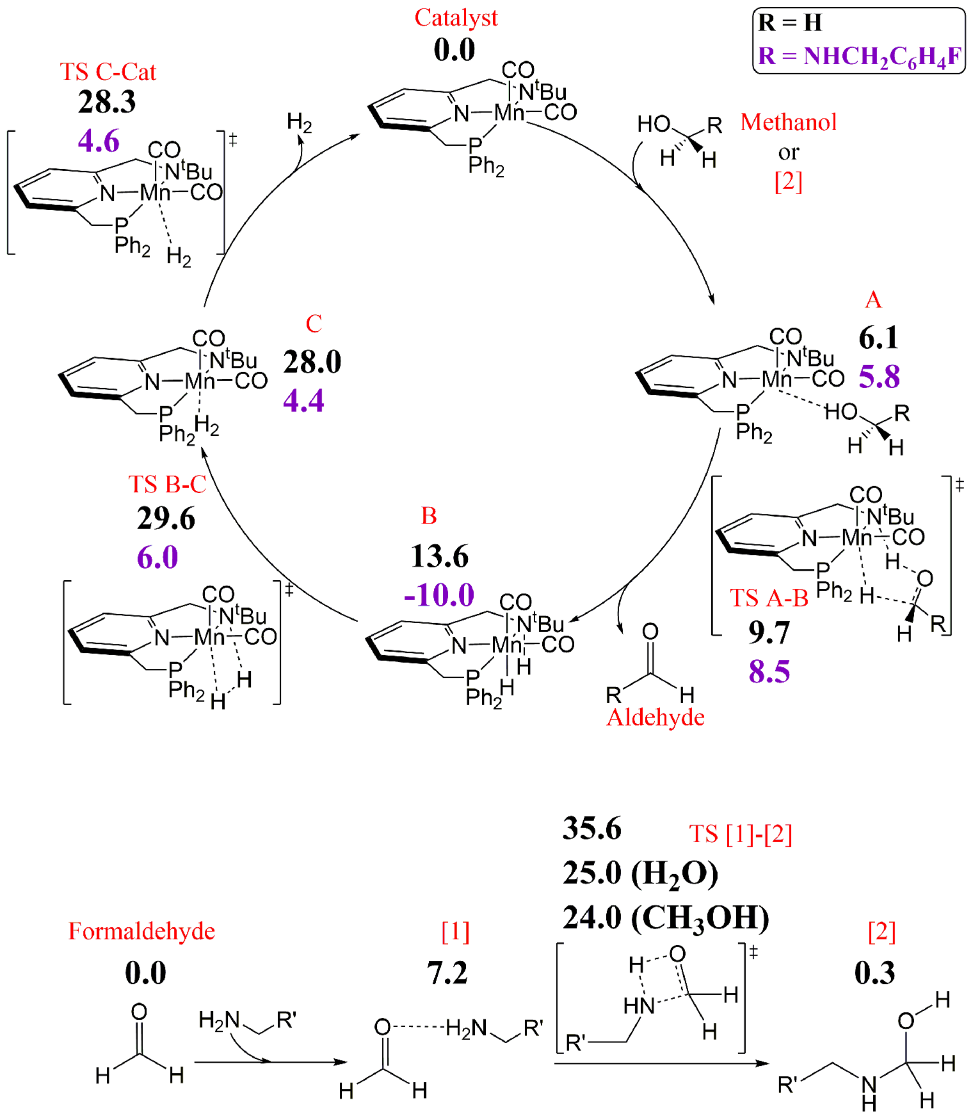

Figure 3. Full mechanism of catalyst **I**. The top cycle shows the aldehyde formation from methanol (black) and hemiaminal [**2**] (magenta). The bottom pathway shows the formation of hemiaminal [**2**] from aldehyde (relative Gibbs energies in kcal/mol).

RESULTS AND DISCUSSION

The mechanism of the reaction of alcohols with amines to form amides in the presence of catalyst **1** is shown in Figure 3. The first step includes the formation of the adduct **A** between the metal complex with an alcohol molecule, with a destabilizing Gibbs energy of 6.1 kcal/mol. The next step is a concerted double hydrogen transfer from methanol to the catalyst. In detail, one hydrogen atom goes directly to the metal and the other to the N^{t}Bu group bonded to the metal itself, leading to intermediate **B**. This last step, with methanol as alcohol, allows at the same time the release of a molecule of formaldehyde. This process is barrierless in the Gibbs energy surface and has a thermodynamic cost 13.6 kcal/mol with respect to the initial catalyst. Then, reductive elimination in **B** leads to the formation of H_2 coordinated to manganese. This reductive elimination involves the upper energy point of the catalytic cycle, with a value of 29.6 kcal/mol from the TDI that is the initial catalyst to the TDTS,[42] 16.0 kcal/mol from **B**, forming a relatively unstable intermediate **C**. In the next step, **C** overcomes an insignificant energy barrier of 0.3 kcal/mol to release H_2 and regenerate the catalyst. Thermodynamically, the whole catalytic cycle releases 10.3 kcal/mol, whereas kinetically, the formation of intermediate **C** defines the rate-determining step (RDS) with the overall cost of 29.6 kcal/mol (see Figure 4a). This is in agreement with the experimental temperature of 383.15 K. In addition, even though the energy difference is not that significant, the substitution in *para* of the pyridyl group by NH_2 and CN groups modified this energy barrier to 29.4 and 29.7 kcal/mol, respectively, showing that an electron-donating group in this position of the ring slightly facilitates overcoming the energy barrier of the RDS.

Once the first catalytic cycle finishes and formaldehyde appears in the media, there is a combination of formaldehyde, obtained in the first catalytic cycle, with amine, and thus the nonmetal-catalyzed pathway starts. It is a simple reaction of formaldehyde with the amine, which develops into hemiaminal [**2**]. The corresponding energy barrier is high (35.6 kcal/mol), but when assisted by an explicit molecule of methanol, the energy barrier is lowered by 11.6−24.0 kcal/mol (see Figure 4b,c). Even though this barrier is relatively high, it does not dispute the RDS through **TS B-C** of the initial catalytic cycle.[42] Once [**2**] is formed, it enters the second catalytic cycle when

https://doi.org/10.1021/acscatal.1c00693
ACS Catal. 2021, 11, 6155−6161

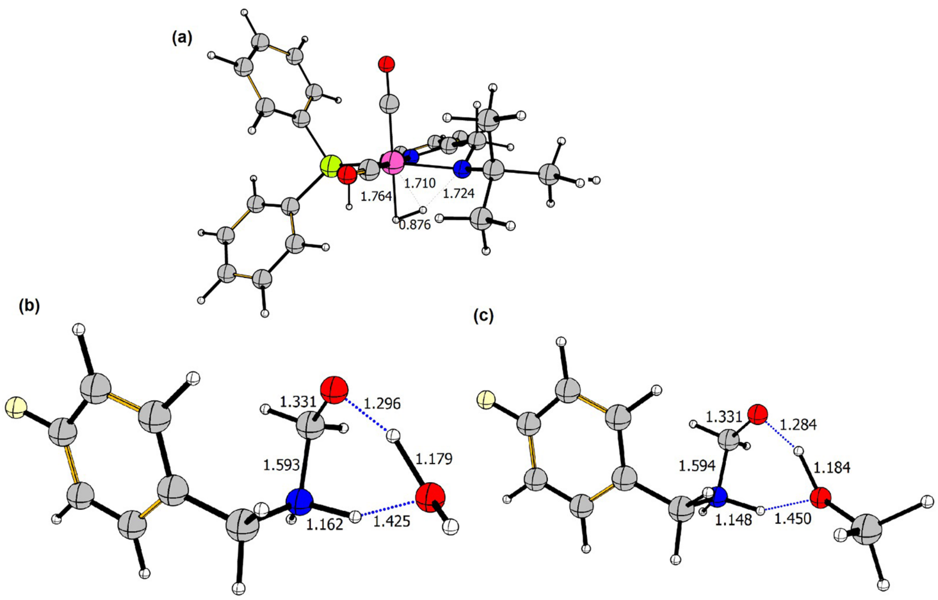

Figure 4. Transition states (a) **B** → **C**, (b) [**1**] → [**2**] (assisted by water), and (c) [**1**] → [**2**] (assisted by methanol); selected distances given in Å.

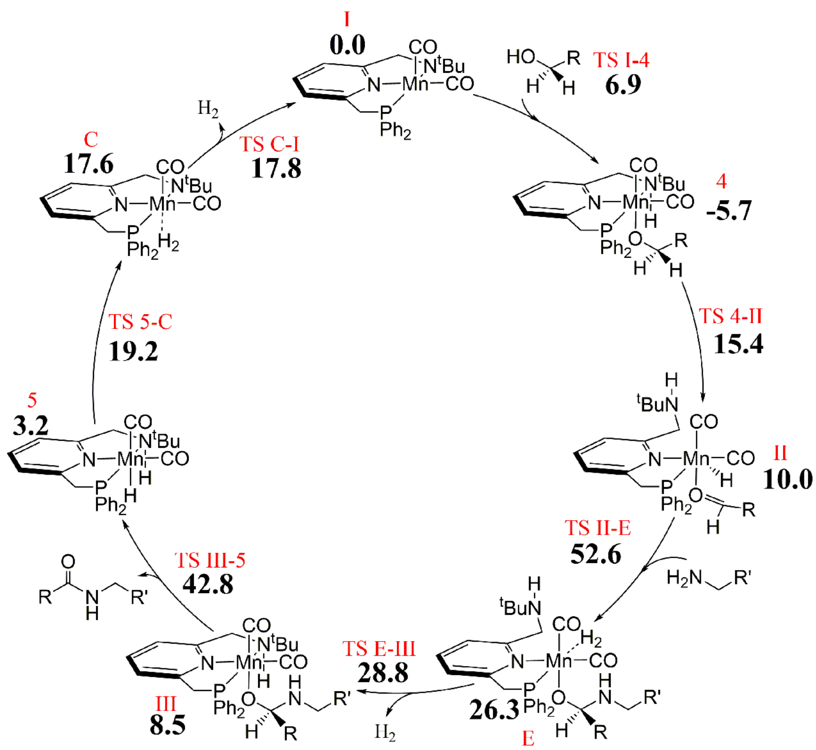

Figure 5. Alternative mechanism of catalyst **1** incorporating the Mn−N bond cleavage (relative Gibbs energies in kcal/mol).

combined with catalyst **I**. The steps are mimetic of those found in the first catalytic cycle. Despite the analogies, there are certain differences. Specifically, **TS A-B** is 1.4 kcal/mol lower for [**2**] than for methanol, and the following steps are considerably less kinetically demanding. Actually, the RDS previously described by **TS B-C** requires only 16.0 kcal/mol in this second catalytic pathway, taking now **B** as the TDI, instead of the initial catalyst for the first catalytic pathway.

Overall, the above mechanism is comprised by (1) synthesis of formaldehyde from methanol, (2) formation of hemiaminal [**2**] from formaldehyde, and (3) synthesis of the product from compound [**2**]. We call this mechanism a "double carrousel" because it first synthesizes an aldehyde from alcohol, and then, it forms compound [**2**], a second alcohol that restarts the initial catalytic cycle. Consequently, it repeats the catalytic mechanism twice. Completing the double carrousel gives two hydrogen molecules, which complies with the experimental finding of 1.7 equiv compared to either the amine or the alcohol.

To have absolute certainty of having recognized the correct mechanism, we still need to compare it to the initial guess (Figure 2) to find out why this mechanism was not plausible even though the cleavage of a Mn−N bond does not require the presence of a nonmetal-catalyzed step. DFT calculations of the hypothesized mechanism in Figure 5 rule out the existence of this alternative mechanism.

Starting from catalyst **I**, the methanol molecule attacks the metal center via the oxygen atom, leading to intermediate **4**, once the hydroxyl transfers its hydrogen to the N^tBu moiety. This step is easy to achieve since the energy barrier is only 6.9 kcal/mol. Next, there are two concerted transformations before reaching compound **II**. First, we must open the $Mn-N^tBu$ bond, with a calculated energy barrier of 21.1 kcal/mol. Then, there is a hydrogen transfer from the former alcohol leading to the formation of a hydride. In complex **II**, there is an agostic interaction of the closest methylenic hydrogen with the metal that provides some additional stabilization of this complex. This last hydrogen transfer facilitates the attack of the amine on the newly dehydrated carbon (**TS II-E**), which involves the formation of H_2 on the metal. It is defined as the RDS of this alternative reaction pathway, with a kinetic cost of 52.6 kcal/mol when assisted by a water molecule. The next release of a hydrogen molecule again has a low cost as in the mechanism of Figure 3, specifically 2.5 kcal/mol, and has a very favorable thermodynamics of 17.8 kcal/mol, partly justified by the coordination of the labile arm previously dissociated from the metal. But this step precedes an expensive transfer of hydrogen to the metal as a hydride (42.8 kcal/mol from initial catalyst **I**) to release the amide product. Final reductive elimination in **5** releases the second molecule of hydrogen and regenerates initial catalyst **I**. Either way, the energy barrier for the RDS is insurmountable under the reaction conditions. Thus, this alternative pathway is not the optimal pathway for the catalyst, not for the initial or final steps, but for the RDS that occurs once the Mn−N bond is broken.[43] Thus, in consistency with the past ruthenium-based catalyst, Mn catalysis involving a hemilabile pincer amine arm is found to be not feasible.[44]

■ CONCLUSIONS

The mechanism for the dehydrogenative amide synthesis from alcohols and amines has been studied with DFT calculations. The most plausible reaction mechanism found involves a double-carrousel catalytic cycle to get aldehydes twice, first, the reagent aldehyde in the metal-catalyzed cycle, and second, the product aldehyde (the amide) from the hemiaminal generated by the combination of formaldehyde and amine in a nonmetal-catalyzed step. Thus, the reaction mechanism is divided into aldehyde synthesis and hemiaminal formation, metal- and nonmetal-catalyzed, respectively. The overall RDS appears at the hydrogen formation (29.6 kcal/mol), thus in the metal-catalyzed cycle, whereas the most energetically demanding nonmetal-catalyzed step unveils a rather high kinetic cost (24.0 kcal/mol) as well. An alternative mechanism, in which all steps are catalyzed by the metal and which involves the breaking of a Mn−N bond, was found unrealistic under the experimental conditions.

■ ASSOCIATED CONTENT

Supporting Information

The Supporting Information is available free of charge at https://pubs.acs.org/doi/10.1021/acscatal.1c00693.

Computational details and all *XYZ* coordinates, absolute energies, and 3D structures of all species (XYZ)

■ AUTHOR INFORMATION

Corresponding Authors

Miquel Solà − *Institut de Química Computacional i Catàlisi and Departament de Química, Universitat de Girona, 17003 Girona, Catalonia, Spain;* orcid.org/0000-0002-1917-7450; Email: miquel.sola@udg.edu

Albert Poater − *Institut de Química Computacional i Catàlisi and Departament de Química, Universitat de Girona, 17003 Girona, Catalonia, Spain;* orcid.org/0000-0002-8997-2599; Email: albert.poater@udg.edu

Authors

Jesús A. Luque-Urrutia − *Institut de Química Computacional i Catàlisi and Departament de Química, Universitat de Girona, 17003 Girona, Catalonia, Spain*

Tània Pèlachs − *Institut de Química Computacional i Catàlisi and Departament de Química, Universitat de Girona, 17003 Girona, Catalonia, Spain*

Complete contact information is available at:
https://pubs.acs.org/10.1021/acscatal.1c00693

Notes

The authors declare no competing financial interest.

■ ACKNOWLEDGMENTS

J.A.L.-U. thanks Universitat de Girona for an IFUdG2017 Ph.D. fellowship. A.P. is a Serra Húnter Fellow. A.P. and M.S. thank the Ministerio de Economía y Competitividad (MINECO) of Spain for projects PGC2018-097722-B-I00 and CTQ2017-85341-P and the Generalitat de Catalunya for project 2017SGR39 and ICREA Academia prize 2019 to A.P. The authors thank Prof. David Milstein for helpful discussion, especially centered on the hemilability of the pincer ligand.

■ REFERENCES

(1) Knobloch, F.; Hanssen, S. V.; Lam, A.; Pollitt, H.; Salas, P.; Chewpreecha, U.; Huijbregts, M. A. J.; Mercure, J.-F. Net emission Reductions From Electric Cars and Heat Pumps in 59 World Regions Over Time. *Nat. Sustainability* **2020**, *3*, 437−447.

(2) López, J. C.; Quijano, G.; Souza, T. S. O.; Estrada, J. M.; Lebrero, R.; Muñoz, R. Biotechnologies for Greenhouse Gases (CH_4, N_2O, and CO_2) Abatement: State of the Art and Challenges. *Appl. Microbiol. Biotechnol.* **2013**, *97*, 2277−2303.

(3) Portmann, R. W.; Daniel, J. S.; Ravishankara, A. R. Research Stratospheric Ozone Depletion due to Nitrous Oxide: Influences of other Gases. *Philos. Trans. R. Soc. B* **2012**, *367*, 1256−1264.

(4) (a) Freedman, B.; Frost, R. *Gale Encyclopedia of Science*; Gale Group, 1995; pp 1875−1880. (b) Rodhe, H. A Comparison of the Contribution of Various Greenhouse Gases to the Greenhouse Effect. *Science* **1990**, *248*, 1217−1219.

(5) (a) Konsolakis, M. Recent Advances on Nitrous Oxide (N_2O) Decomposition over Non-Noble-Metal Oxide Catalysts: Catalytic Performance, Mechanistic Considerations, and Surface Chemistry Aspects. *ACS Catal.* **2015**, *5*, 6397−6421. (b) Severin, K. Synthetic Chemistry with Nitrous Oxide. *Chem. Soc. Rev.* **2015**, *44*, 6375−6386. (c) Parmon, V. N.; Panov, G. I.; Uriarte, A.; Noskov, A. S. Nitrous Oxide in Oxidation Chemistry and Catalysis: Application and Production. *Catal. Today* **2005**, *100*, 115−131. (d) Tolman, W. B. Binding and Activation of N_2O at Transition Metal Centers: Recent Mechanistic Insight. *Angew. Chem., Int. Ed.* **2010**, *49*, 1018−1024.

(6) (a) Hsu, J.; Prather, M. J. Global Long-Lived Chemical Modes Excited in a 3-D Chemistry Transport Model: Stratospheric N_2O, NO_y, O_3 and CH_4 Chemistry. *Geophys. Res. Lett.* **2010**, *37*, No. L07805. (b) Montzka, S. A.; Dlugokencky, E. J.; Butler, J. H. Non-CO_2 Greenhouse Gases and Climate Change. *Nature* **2011**, *476*,

43−50. (c) Prather, M. J.; Hsu, J.; DeLuca, N. M.; Jackman, C. H.; Oman, L. D.; Douglass, A. R.; Fleming, E. L.; Strahan, S. S.; Steenrod, S. D.; Søvde, O. A.; Isaksen, I. S. A.; Froidevaux, L.; Funke, B. Measuring and Modeling the Lifetime of Nitrous Oxide Including its Variability. *J. Geophys. Res.* **2015**, *120*, 5693−5705.

(7) (a) Zeng, R.; Feller, M.; Ben-David, Y.; Milstein, D. Hydrogenation and Hydrosilylation of Nitrous Oxide Homogeneously Catalyzed by a Metal Complex. *J. Am. Chem. Soc.* **2017**, *139*, 5720−5723. (b) Pal, T. K.; De, D.; Bharadwaj, P. K. Metal-organic Frameworks for the Chemical Fixation of CO_2 into Cyclic Carbonates. *Coord. Chem. Rev.* **2020**, *408*, No. 213173. (c) Zeng, R.; Feller, M.; Diskin-Posner, Y.; Shimon, L. J. W.; Ben-David, Y.; Milstein, D. CO Oxidation by N_2O Homogeneously Catalyzed by Ruthenium Hydride Pincer Complexes Indicating a New Mechanism. *J. Am. Chem. Soc.* **2018**, *140*, 7061−7064.

(8) (a) Luque-Urrutia, J. A.; Poater, A. The Fundamental non Innocent Role of Water for the Hydrogenation of Nitrous Oxide by PNP Pincer Ru-based Catalysts. *Inorg. Chem.* **2017**, *56*, 14383−14387. (b) Escayola, S.; Solà, M.; Poater, A. Mechanism of the Facile Nitrous Oxide Fixation by Homogeneous Ruthenium Hydride Pincer Catalysts. *Inorg. Chem.* **2020**, *59*, 9374−9383.

(9) (a) Maity, B.; Koley, D. Computational Investigation on the Role of Disilene Substituents Toward N_2O Activation. *J. Phys. Chem. A* **2017**, *121*, 401−417. (b) Wendel, D.; Szilvási, T.; Henschel, D.; Altmann, P. J.; Jandl, C.; Inoue, S.; Rieger, B. Precise Activation of Ammonia and Carbon Dioxide by an Iminodisilene. *Angew. Chem., Int. Ed.* **2018**, *57*, 14575−14579. (c) Sodpiban, O.; Del Gobbo, S.; Barman, S.; Aomchad, V.; Kidkhunthod, P.; Ould-Chikh, S.; Poater, A.; D'Elia, V.; Basset, J.-M. Synthesis of Well-defined Yttrium-based Lewis Acids by Capture of a Reaction Intermediate and Catalytic Application for Cycloaddition of CO_2 to Epoxides Under Atmospheric Pressure. *Catal. Sci. Technol.* **2019**, *9*, 6152−6165. (d) Coufourier, S.; Gaignard-Gaillard, Q.; Lohier, J.-F.; Poater, A.; Gaillard, S.; Renaud, J.-L. Hydrogenation of CO_2, Hydrogenocarbonate, and Carbonate to Formate in Water using Phosphine Free Bifunctional Iron Complexes. *ACS Catal.* **2020**, *10*, 2108−2116. (e) Sarkar, D.; Weetman, C.; Dutta, S.; Schubert, E.; Jandl, C.; Koley, D.; Inoue, S. N-Heterocyclic Carbene-Stabilized Germa-acylium Ion: Reactivity and Utility in Catalytic CO_2 Functionalizations. *J. Am. Chem. Soc.* **2020**, *142*, 15403−15411.

(10) (a) Crabtree, R. H. Homogeneous Transition Metal Catalysis of Acceptorless Dehydrogenative Alcohol Oxidation: Applications in Hydrogen Storage and to Heterocycle Synthesis. *Chem. Rev.* **2017**, *117*, 9228−9246. (b) Gunanathan, C.; Milstein, D. Applications of Acceptorless Dehydrogenation and Related Transformations in Chemical Synthesis. *Science* **2013**, *341*, No. 1229712.

(11) (a) Das, U. K.; Chakraborty, S.; Diskin-Posner, Y.; Milstein, D. Direct Conversion of Alcohols into Alkenes by Dehydrogenative Coupling with Hydrazine/Hydrazone Catalyzed by Manganese. *Angew. Chem., Int. Ed.* **2018**, *57*, 13444−13448. (b) Azofra, L. M.; Poater, A. Diastereoselective diazenyl formation: the key for manganese-catalysed alcohol conversion into (E)-alkenes. *Dalton Trans.* **2019**, *48*, 14122−14127.

(12) Mukherjee, A.; Nerush, A.; Leitus, G.; Shimon, L. J. W.; David, Y. B.; Jalapa, N. A. E.; Milstein, D. Manganese-Catalyzed Environmentally Benign Dehydrogenative Coupling of Alcohols and Amines to Form Aldimines and H_2: A Catalytic and Mechanistic Study. *J. Am. Chem. Soc.* **2016**, *138*, 4298−4301.

(13) (a) Kumar, A.; Espinosa-Jalapa, N. A.; Leitus, G.; Diskin-Posner, Y.; Avram, L.; Milstein, D. Direct Synthesis of Amides by Dehydrogenative Coupling of Amines with either Alcohols or Esters: Manganese Pincer Complex as Catalyst. *Angew. Chem., Int. Ed.* **2017**, *56*, 14992−14996. (b) Masdemont, J.; Luque-Urrutia, J. A.; Gimferrer, M.; Milstein, D.; Poater, A. Mechanism of Coupling of Alcohols and Amines to Generate Aldimines and H_2 by a Pincer Manganese Catalyst. *ACS Catal.* **2019**, *9*, 1662−1669.

(14) (a) Chakraborty, S.; Das, U. K.; Ben-David, Y.; Milstein, D. Manganese Catalyzed α-Olefination of Nitriles by Primary Alcohols. *J. Am. Chem. Soc.* **2017**, *139*, 11710−11713. (b) Chakraborty, S.; Gellrich, U.; Diskin-Posner, Y.; Leitus, G.; Avram, L.; Milstein, D. Manganese-Catalyzed N-Formylation of Amines by Methanol Liberating H_2: A Catalytic and Mechanistic Study. *Angew. Chem., Int. Ed.* **2017**, *56*, 4229−4233.

(15) Luque-Urrutia, J. A.; Solà, M.; Milstein, D.; Poater, A. Mechanism of the Manganese-Pincer Catalyzed Acceptorless Dehydrogenative Coupling of Nitriles and Alcohols. *J. Am. Chem. Soc.* **2019**, *141*, 2398−2403.

(16) (a) Barta, K.; Ford, P. C. Catalytic Conversion of Nonfood Woody Biomass Solids to Organic Liquids. *Acc. Chem. Res.* **2014**, *47*, 1503−1512. (b) Vispute, T. P.; Zhang, H.; Sanna, A.; Xiao, R.; Huber, G. W. Renewable Chemical Commodity Feedstocks From Integrated Catalytic Processing of Pyrolysis Oils. *Science* **2010**, *330*, 1222−1227.

(17) Kumar, A.; Janes, T.; Espinosa-Jalapa, N. A.; Milstein, D. Selective Hydrogenation of Cyclic Imides to Diols and Amines and Its Application in the Development of a Liquid Organic Hydrogen Carrier. *J. Am. Chem. Soc.* **2018**, *140*, 7453−7457.

(18) Zhang, J.; Leitus, G.; Ben-David, Y.; Milstein, D. Facile Conversion of Alcohols into Esters and Dihydrogen Catalyzed by New Ruthenium Complexes. *J. Am. Chem. Soc.* **2005**, *127*, 10840−10841.

(19) Gunanathan, C.; Ben-David, Y.; Milstein, D. Direct Synthesis of Amides from Alcohols and Amines with Liberation of H_2. *Science* **2007**, *317*, 790−792.

(20) (a) Gunanathan, C.; Milstein, D. Metal-Ligand Cooperation by Aromatization-Dearomatization: A New Paradigm in Bond Activation and "Green" Catalysis. *Acc. Chem. Res.* **2011**, *44*, 588−602. (b) Zhang, J.; Balaraman, E.; Leitus, G.; Milstein, D. Electron-Rich PNP- and PNN-Type Ruthenium(II) Hydrido Borohydride Pincer Complexes. Synthesis, Structure, and Catalytic Dehydrogenation of Alcohols and Hydrogenation of Esters. *Organometallics* **2011**, *30*, 5716−5724. (c) Gnanaprakasam, B.; Milstein, D. Synthesis of Amides from Esters and Amines with Liberation of H_2 under Neutral Conditions. *J. Am. Chem. Soc.* **2011**, *133*, 1682−1685.

(21) Jin, H.; Xie, J.; Pan, C.; Zhu, Z.; Cheng, Y.; Zhu, C. Rhenium-Catalyzed Acceptorless Dehydrogenative Coupling via Dual Activation of Alcohols and Carbonyl Compounds. *ACS Catal.* **2013**, *3*, 2195−2198.

(22) (a) Mastalir, M.; Tomsu, G.; Pittenauer, E.; Allmaier, G.; Kirchner, K. Co(II) PCP Pincer Complexes as Catalysts for the Alkylation of Aromatic Amines with Primary Alcohols. *Org. Lett.* **2016**, *18*, 3462−3465. (b) Mastalir, M.; Glatz, M.; Gorgas, N.; Stöger, B.; Pittenauer, E.; Allmaier, G.; Veiros, L. F.; Kirchner, K. Divergent Coupling of Alcohols and Amines Catalyzed by Isoelectronic Hydride Mn^{I} and Fe^{II} PNP Pincer Complexes. *Chem. − Eur. J.* **2016**, *22*, 12316−12320. (c) Lane, E. M.; Hazari, N.; Bernskoetter, W. H. Iron-Catalyzed Urea Synthesis: Dehydrogenative Coupling of Methanol and Amines. *Chem. Sci.* **2018**, *9*, 4003−4008. (d) Mukherjee, A.; Milstein, D. Homogeneous Catalysis by Cobalt and Manganese Pincer Complexes. *ACS Catal.* **2018**, *8*, 11435−11469. (e) Alig, L.; Fritz, M.; Schneider, S. First-Row Transition Metal (De)-Hydrogenation Catalysis Based on Functional Pincer Ligands. *Chem. Rev.* **2019**, *119*, 2681−2751. (f) Jayarathne, U.; Zhang, Y.; Hazari, N.; Bernskoetter, W. H. Selective Iron-Catalyzed Deaminative Hydrogenation of Amides. *Organometallics* **2017**, *36*, 409−416.

(23) (a) Waiba, S.; Maji, B. Manganese Catalyzed Acceptorless Dehydrogenative Coupling Reactions. *ChemCatChem* **2020**, *12*, 1891−1902. (b) Chandra, P.; Ghosh, T.; Choudhary, N.; Mohammad, A.; Mobin, S. M. Recent Advancement in Oxidation or Acceptorless Dehydrogenation of Alcohols to Valorised Products Using Manganese Based Catalysts. *Coord. Chem. Rev.* **2020**, *411*, No. 213241. (c) Borghs, J. C.; Azofra, L. M.; Biberger, T.; Linnenberg, O.; Cavallo, L.; Rueping, M.; El-Sepelgy, O. Manganese-Catalyzed Multicomponent Synthesis of Pyrroles through Acceptorless Dehydrogenation Hydrogen Autotransfer Catalysis: Experiment and Computation. *ChemSusChem* **2019**, *12*, 3083−3088.

(24) (a) van Koten, G.; Milstein, D. *Organometallic Pincer Chemistry*; Springer-Verlag: Berlin, 2013. (b) Peris, E.; Crabtree, R. H. Key

Factors in Pincer Ligand Design. *Chem. Soc. Rev.* **2018**, *47*, 1959−1968.

(25) (a) Bray, B. L. Large-Scale Manufacture of Peptide Therapeutics by Chemical Synthesis. *Nat. Rev. Drug Discovery* **2003**, *2*, 587−593. (b) Carey, J. S.; Laffan, D.; Thomson, C.; Williams, M. T. Analysis of the Reactions Used for the Preparation of Drug Candidate Molecules. *Org. Biomol. Chem.* **2006**, *4*, 2337−2347. (c) Dunetz, J. R.; Magano, J.; Weisenburger, G. A. Large-Scale Applications of Amide Coupling Reagents for the Synthesis of Pharmaceuticals. *Org. Process Res. Dev.* **2016**, *20*, 140−177.

(26) Cupido, T.; Tulla-Puche, J.; Spengler, J.; Albericio, F. The Synthesis of Naturally Occurring Peptides and their Analogs. *Curr. Opin. Drug Discovery Dev.* **2007**, *10*, 768−783.

(27) Constable, D. J. C.; Dunn, P. J.; Hayler, J. D.; Humphrey, G. R.; Leazer, J. L., Jr.; Linderman, R. J.; Lorenz, K.; Manley, J.; Pearlman, B. A.; Wells, A.; Zaks, A.; Zhang, T. Y. Key Green Chemistry Research Areas—a Perspective from Pharmaceutical Manufacturers. *Green Chem.* **2007**, *9*, 411−420.

(28) (a) Basha, A.; Lipton, M.; Weinreb, S. M. A Mild, General Method for Conversion of Esters to Amides. *Tetrahedron Lett.* **1977**, *18*, 4171−4174. (b) Wang, W.-B.; Roskamp, E. J. Tin(II) Amides: New Reagents for the Conversion of Esters to Amides. *J. Org. Chem.* **1992**, *57*, 6101−6103. (c) Williams, J. M.; Jobson, R. B.; Yasuda, N.; Marchesini, G.; Dolling, U.-H.; Grabowski, E. J. J. A New General Method for Preparation of N-methoxy-N-methylamides. Application in Direct Conversion of an Ester to a Ketone. *Tetrahedron Lett.* **1995**, *36*, 5461−5464.

(29) (a) Han, S.-Y.; Kim, Y.-A. Recent Development of Peptide Coupling Reagents in Organic Synthesis. *Tetrahedron* **2004**, *60*, 2447−2467. (b) Valeur, E.; Bradley, M. Amide Bond Formation: Beyond the Myth of Coupling Reagents. *Chem. Soc. Rev.* **2009**, *38*, 606−631. (c) de Figueiredo, R. M.; Suppo, J.-S.; Campagne, J.-M. Nonclassical Routes for Amide Bond Formation. *Chem. Rev.* **2016**, *116*, 12029−12122.

(30) Espinosa-Jalapa, N. A.; Kumar, A.; Leitus, G.; Diskin-Posner, Y.; Milstein, D. Synthesis of Cyclic Imides by Acceptorless Dehydrogenative Coupling of Diols and Amines Catalyzed by a Manganese Pincer Complex. *J. Am. Chem. Soc.* **2017**, *139*, 11722−11725.

(31) Frisch, M. J.; Trucks, G. W.; Schlegel, H. B.; Scuseria, G. E.; Robb, M. A.; Cheeseman, J. R.; Scalmani, G.; Barone, V.; Petersson, G. A.; Nakatsuji, H.; Li, X.; Caricato, M.; Marenich, A. V.; Bloino, J.; Janesko, B. G.; Gomperts, R.; Mennucci, B.; Hratchian, H. P.; Ortiz, J. V.; Izmaylov, A. F.; Sonnenberg, J. L.; Williams-Young, D.; Ding, F.; Lipparini, F.; Egidi, F.; Goings, J.; Peng, B.; Petrone, A.; Henderson, T.; Ranasinghe, D.; Zakrzewski, V. G.; Gao, J.; Rega, N.; Zheng, G.; Liang, W.; Hada, M.; Ehara, M.; Toyota, K.; Fukuda, R.; Hasegawa, J.; Ishida, M.; Nakajima, T.; Honda, Y.; Kitao, O.; Nakai, H.; Vreven, T.; Throssell, K.; Montgomery Jr, J. A.; Peralta, J. E.; Ogliaro, F.; Bearpark, M. J.; Heyd, J. J.; Brothers, E. N.; Kudin, K. N.; Staroverov, V. N.; Keith, T. A.; Kobayashi, R.; Normand, J.; Raghavachari, K.; Rendell, A. P.; Burant, J. C.; Iyengar, S. S.; Tomasi, J.; Cossi, M.; Millam, J. M.; Klene, M.; Adamo, C.; Cammi, R.; Ochterski, J. W.; Martin, R. L.; Morokuma, K.; Farkas, O.; Foresman, J. B.; Fox, D. J. *Gaussian 16*, revision C.01; Gaussian, Inc.: Wallingford, CT, 2016.

(32) (a) Becke, A. Density-Functional Exchange-Energy Approximation with Correct Asymptotic Behaviour. *Phys. Rev. A* **1988**, *38*, No. 3098. (b) Perdew, J. P. Density-Functional Approximation for the Correlation Energy of the Inhomogeneous Electron Gas. *Phys. Rev. B* **1986**, *33*, No. 8822. (c) Perdew, J. P. Erratum: Density-functional Approximation for the Correlation Energy of the Inhomogeneous Electron Gas. *Phys. Rev. B* **1986**, *34*, No. 7406.

(33) (a) Weigend, F.; Ahlrichs, R. Balanced Basis Sets of Split Valence, Triple Zeta Valence and Quadruple Zeta Valence Quality for H to Rn: Design and Assessment of Accuracy. *Phys. Chem. Chem. Phys.* **2005**, *7*, 3297−3305. (b) Weigend, F. Accurate Coulomb-fitting basis sets for H to Rn. *Phys. Chem. Chem. Phys.* **2006**, *8*, 1057−1065.

(34) Johnson, E. R.; Becke, A. D. A Post-Hartree-Fock Model of Intermolecular Interactions: Inclusion of Higher-Order Corrections. *J. Chem. Phys.* **2006**, *124*, No. 174104.

(35) (a) Grimme, S.; Antony, J.; Ehrlich, S.; Krieg, H. A Consistent and Accurate Ab Initio Parametrization of Density Functional Dispersion Correction (DFT-D) for the 94 Elements H-Pu. *J. Chem. Phys.* **2010**, *132*, No. 154104. (b) Grimme, S.; Ehrlich, S.; Goerigk, L. Effect of the Damping Function in Dispersion Corrected Density Functional Theory. *J. Comput. Chem.* **2011**, *32*, 1456−1465.

(36) (a) Barone, V.; Cossi, M. Quantum Calculation of Molecular Energies and Energy Gradients in Solution by a Conductor Solvent Model. *J. Phys. Chem. A* **1998**, *102*, 1995−2001. (b) Tomasi, J.; Persico, M. Molecular Interactions in Solution: An Overview of Methods Based on Continuous Distributions of the Solvent. *Chem. Rev.* **1994**, *94*, 2027−2094.

(37) Zhao, Y.; Truhlar, D. G. The M06 Suite of Density Functionals for Main Group Thermochemistry, Thermochemical Kinetics, Noncovalent Interactions, Excited States, and Transition Elements: Two New Functionals and Systematic Testing of Four M06-Class Functionals and 12 Other Functionals. *Theor. Chem. Acc.* **2008**, *120*, 215−241.

(38) Kendall, R. A.; Dunning, T. H., Jr.; Harrison, R. J. Electron Affinities of the First-Row Atoms Revisited. Systematic Basis Sets and Wave Functions. *J. Chem. Phys.* **1992**, *96*, 6796−6806.

(39) (a) Leitgeb, A.; Abbas, M.; Fischer, R. C.; Poater, A.; Cavallo, L.; Slugovc, C. A latent Ruthenium Based Olefin Metathesis Catalyst with a Sterically Demanding NHC Ligand (Pre)Catalysts. *Catal. Sci. Technol.* **2012**, *2*, 1640−1643. (b) Lator, A.; Gaillard, S.; Poater, A.; Renaud, J.-L. Iron-Catalyzed Chemoselective Reduction of α,β-Unsaturated Ketones. *Chem. − Eur. J.* **2018**, *24*, 5770−5774. (c) Gómez-Suárez, A.; Oonishi, Y.; Martin, A. R.; Vummaleti, S. V. C.; Nelson, D. J.; Cordes, D. B.; Slawin, A. M. Z.; Cavallo, L.; Nolan, S. P.; Poater, A. On the Mechanism of the Digold(I)-Hydroxide-Catalysed Hydrophenoxylation of Alkynes. *Chem. − Eur. J.* **2016**, *22*, 1125−1132. (d) Poater, A.; Pump, E.; Vummaleti, S. V. C.; Cavallo, L. The Right Computational Recipe for Olefin Metathesis with Ru-based Catalysts: the Whole Mechanism of Ring-Closing Olefin Metathesis. *J. Chem. Theory Comput.* **2014**, *10*, 4442−4448.

(40) Besora, M.; Vidossich, P.; Lledós, A.; Ujaque, G.; Maseras, F. Calculation of Reaction Free Energies in Solution: A Comparison of Current Approaches. *J. Phys. Chem. A* **2018**, *122*, 1392−1399.

(41) (a) Kelly, C. P.; Cramer, C. J.; Truhlar, D. G. SM6: A Density Functional Theory Continuum Solvation Model for Calculating Aqueous Solvation Free Energies of Neutrals, Ions, and Solute−Water Clusters. *J. Chem. Theory Comput.* **2005**, *1*, 1133−1152. (b) Kelly, C. P.; Cramer, C. J.; Truhlar, D. G. Aqueous Solvation Free Energies of Ions and Ion−Water Clusters Based on an Accurate Value for the Absolute Aqueous Solvation Free Energy of the Proton. *J. Phys. Chem. B* **2006**, *110*, 16066−16081. (c) Bryantsev, V. S.; Diallo, M. S.; Goddard, W. A., III Calculation of Solvation Free Energies of Charged Solutes Using Mixed Cluster/Continuum Models. *J. Phys. Chem. B* **2008**, *112*, 9709−9719.

(42) Kozuch, S.; Shaik, S. How to Conceptualize Catalytic Cycles? The Energetic Span Model. *Acc. Chem. Res.* **2011**, *44*, 101−110.

(43) Li, H.; Hall, M. B. Computational Mechanistic Studies on Reactions of Transition Metal Complexes with Noninnocent Pincer Ligands: Aromatization−Dearomatization or Not. *ACS Catal.* **2015**, *5*, 1895−1913.

(44) Nguyen, D. H.; Trivelli, X.; Capet, F.; Paul, J.-F.; Dumeignil, F.; Gauvin, R. M. Manganese Pincer Complexes for the Base-Free, Acceptorless Dehydrogenative Coupling of Alcohols to Esters: Development, Scope, and Understanding. *ACS Catal.* **2017**, *7*, 2022−2032.